Research Article GU J Sci 31(4): 1229-1244 (2018)

Gazi University

Journal of Science

http://dergipark.gov.tr/gujs

Thermal Analysis of Chip on Board Packaging of High Power Led's with Heat Pipe Using Cfd for Street Lights

Burcu CICEK[1,*], Necmettin SAHIN[1], Mahmut ALKAN[2]

[1] *Aksaray University, Faculty of Engineering, 68100, Aksaray, Turkey*

[2] *NiğdeÖmerHalisdemir University, Faculty of Engineering,51245, Niğde, Turkey*

Article Info

Received: 30/03/2018
Accepted: 09/07/2018

Keywords

High power led
CFD
Heat pipe
Thermal analysis

Abstract

In this study, in order to provide heat dissipation of the high power LEDs to be used for street illumination, U-shaped cylindrical copper heat pipes are used. Thermal analysis of this system was carried out numerically in the ANSYS Fluent software. Firstly, thermal analysis was performed for different numbers, diameters and lengths of heat pipes and optimum values were obtained. Afterwards, the optimum materials to be used as components of LED packages were determined. In addition, the effect of the power applied to the LED chip and of ambient temperature on the temperature distribution of the whole system was examined.

1. INTRODUCTION

Light emitting diodes (LED's) are solid state semiconductor devices that directly convert electrical energy into light energy; however, LEDs convert only about 20% of the applied electric energy to light energy [1]. The remaining energy is converted into heat energy, causing high temperatures in the LED chips. High heat fluxes in the LEDs limit the reliability, stability and lifetime of them. Especially in high power LEDs, it is necessary to keep the junction temperature below the allowable limit. So, effective thermal management of the LED package is critical to improve LED performance. In recent years, many researchers and high-power LED manufacturers have used different cooling methods for LED chips. One of the main methods is to select optimum materials of LED components to solve high heat flux problem that occurs on the LEDs [2-4]. Besides, controlling the cost in high power LED package design is equally important as effective cooling. It is necessary to avoid expensive cooling methods such as fan or liquid cooling. Phase change is a promising cooling method for electronic devices that produce high heat flux. In this regard, heat pipes, which have high effective heat transfer coefficients, no complicated parts and are therefore maintenance free, are seen as a suitable and cost - effective cooling method for solving the heat problem in LEDs.

In the literature, studies related to usage of heat pipes for electronic device cooling are available [5-9]. In addition to those, many studies that use the methods of computational fluid dynamics to simulate the heat pipes are present.

Carbajal et al. [10] numerically modeled the thermal behavior of a flat heat pipe thermal spread with a 3D-quasi mathematical model. For the vapor phase computations, they used explicit finite element method. At the same time, they obtained the velocity distribution within the vapor core. The numerical

*Corresponding author, e-mail: cicekb@aksaray.edu.tr

results produced by their study revealed that, the high heat dissipation of the vapor phase expedites the heat dissipation and makes the temperature distribution more uniform throughout the process.

Naveenkumar et al. [11] simulated cylindirical heat pipes in CFX software, using various wick structures such as Sintered, V-Groove, Screen Groove and wick thicknesses such as 0.5 mm, 0.75 mm and 1 mm. They preferred silica as the heat pipe material, nickel alloy as the wick material and water, methanol and liquid methanol as the working fluid. Then, they obtained the temperature gradients and coefficients of thermal conductivity for every wick structure, wick thickness and working fluid. In another study, the authors manufactured cylindirical heat pipes with 1 m length and 0.031 m outer radius and conducted experimental studies to determine the surface temperature and vapor temperature in both transient and steady - state conditions. In addition, they performed CFD analyses under steady - state conditions and compared the results with the experimental results [12].

Suresh and Bhramara [13] numerically modeled a pulsating heat pipe, which is a two phase heat exchanger that removes heat from the evaporator region and transmits it to the condenser region, in ANSYS CFX. They used acetone as the working fluid and used a filling ratio of 60%. The boundary conditions for heat flux were 9W to 15W in evaporator region and 7945 W/m^2 in the condenser region. Their heat flux value for the adiabatic region was zero. They observed a drop in the temperature of the acetone within the evaporator and this showed that heat was transmitted into the condenser region. Their findings revealed that, the volumetric air to acetone ratio within the evaporator, condenser and adiabatic regions affect the flow model within the PHP.

Asmaie et al. [14] developed a CFD model to simulate the thermosiphon that provides heat transfer by two phase flow. They used de-ionized water and CuO/water nanofluid as the working fluid. Their results showed that, the heat flux in the nanofluid is 46% higher than that in water. Moreover, they observed that, it was possible to decrease the wall temperature by increasing the nanofluid concentration up to some point and the optimum concentration is 1% by weight. Ashish et al. [15] carried out experimental studies to examine the thermal behavior of heat pipes under different operating conditions. They also performed the same analyses numerically in ANSYS software. They charged the heat pipes with water and CuO + BN hybrid nanoparticles. They searched the effect of heat input, heat pipe slope angle and nanoparticle concentration on thermal resistance and found that CuO + BN / H_2O 2% by volume hybrid nanofluids are quite effective in providing maximum heat transfer.

Lin et al. [16] built a comprehensive physical and mathematical model of miniature oscillating heat pipes to examine the heat transfer mechanisms and capacities of them. They used water as the working fluid. They simulated the MOHP's using volume of fluid (VOF) and mixture models in ANSYS Fluent. Comparison of the outputs from these two models revealed that, mixture model is better for two phase flow simulations. Wang et al. [17] examined 2-D single loop closed-loop pulsating heat pipes (CLPHP) by CFD methods. They used the volume of fluid (VOF) method for computations and they determined the thermal performance of CLPHP for different evaporator length / condenser length ratios, with a heat input of 10 W to 40 W and a filling ratio of 30% to 60%.

Dev and Budania [18] developed a 2D finite element method to analyze the steady-state performances of heat pipes. They applied their finite element models within ANSYS to estimate the temperature distribution throughout the heat pipe. They performed simulations for different heat pipe materials, wick effective thermal conductivities and working fluids and then determined the optimum values for all of those. Elnaggar et al. [19] used U-shaped cylindirical heat pipes for cooling of PC- CPU's. They also integrated fins to the heat pipe. They performed the experiments by assembling the system onto a heat source within a rectangular tunnel and created the forced convection conditions with a fan. They ran the system in steady state under both natural and forced convection conditions to determine the total thermal resistance and coefficient of thermal conductivity. They also simulated the system using ANSYS 10.

In this study, for cooling the LED packages, which are intended to be used for street illumination purposes, 3 U-shaped cylindrical copper heat pipes were installed. The heat pipes consist of three regions, namely, the evaporator region, the adiabatic region and the condenser region. The evaporator region,

which draws heat from the hot medium and transmits it into the condenser, is integrated into the heat sink, which itself is placed on the bottom of the LED chip, where heat generation is maximum. In the condenser region, a heat sink with fins is installed to enable the working fluid to condense and give out heat to ambient through natural convection. Fin structure is formed in such a way to increase the heat transfer surface area. Thermal analysis of the system was performed in ANSYS Fluent software, in different geometries, using different materials and under different boundary conditions. Thus, temperature distribution was obtained for every case.

2. MATERIALS AND METHODS

2.1. Physical Model

As shown in Figure 1, four pieces of 25 W high power COP LED packages were designed for street lights. Each LED package consisted of an InGaN LED chip, an eutectic material, a die, a die attach material, an electronic circuit board and a thermal interface material, respectively. The dimensions and thermal conductivity of the designed LED package are given in Table 1. Properties of the heat pipes placed into heat sink are also given in Table 2.

Water was preferred as a working fluid in U-shaped cylindrical copper heat pipes used in the system. Boundary conditions were assumed to be as follows: Ambient temperature is 35 °C and the wind speed is 0.1 m/s. Heat flux in a LED chip is constant and calculated by Q / Ab. As previously stated, LEDs convert 20% of the applied electrical energy to heat energy and the rest is converted into heat. So, for a 25W LED chip, heat input was assumed to be Q = 25W x 0.80= 20 W. Ab is the surface area of the LED chip and taken as 961625 mm^2.

Table 1. *Dimensions and thermal conductivities of the designed LED package*

<table>
<tr><th></th><th>Width (mm)</th><th>Dimension (mm)</th><th>Material</th><th>Thermal Conductivity (W/m.K)</th></tr>
<tr><td>LED Chip</td><td>0.6</td><td>R=17</td><td>GaN</td><td>130</td></tr>
<tr><td>Metallization</td><td>0.01</td><td>"</td><td>Au-Si eutectic bonding</td><td>27</td></tr>
<tr><td>Die</td><td>0.375</td><td>"</td><td>Silicon</td><td>124</td></tr>
<tr><td>Die-attach</td><td>0.05</td><td>"</td><td>Au-20Sn</td><td>57</td></tr>
<tr><td rowspan="4">Electronic circuit board</td><td>0.3/ 0.38 / 0.3</td><td rowspan="4">19×19</td><td>Al_2O_3 DBC</td><td>24</td></tr>
<tr><td>0.3/ 0.38 / 0.3</td><td>Si_3N_4 AMB</td><td>80</td></tr>
<tr><td>0.3/ 0.64 / 0.3</td><td>AlN DBC</td><td>180</td></tr>
<tr><td>0.127/ 0.075 / 1</td><td>IMS</td><td>1.1</td></tr>
<tr><td>TIM</td><td>0.05</td><td>"</td><td>Thermal İnterface material</td><td>3</td></tr>
<tr><td>Heat sink</td><td>-</td><td>-</td><td>Aluminum</td><td>202</td></tr>
</table>

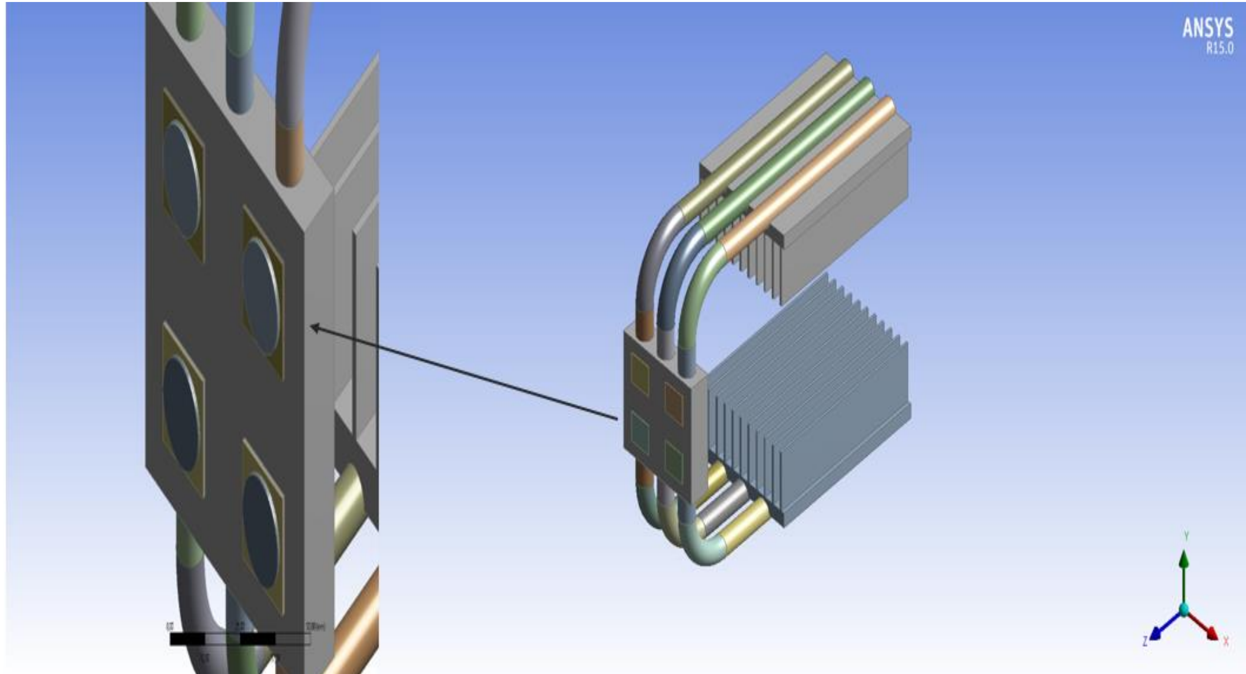

Figure 1. *Geometry of LED package*

Table 2. *Heat pipe properties*

Parameter	
Total heat pipe length	0.58 m
Heat pipe condenser length	0.20 m
Heat pipe evaporator length	0.10 m
Diameter of heat pipe (D)	0.010 m
Material of heat pipe	Copper
Total heat input	25 W
Thermal conductivity of heat pipe	20000 W/m.K
Working Fluid	Water

The initial temperature of heat pipe is determined to be 344 K and standard thermophysical properties of the working fluid at that temperature are added at Table 3.

Table 3. *Thermophysical properties for water*

Description	Liquid	Vapor
Thermal Conductivity (W/m.K)	0.663	0.0221
Density (kg/m^3)	9.77E+2	0.206
Dynamic Viscosity (Pa.s)	3.89E-4	1.13E-5
Specific Heat (J/kg.K)	4.07E+3	1.98E+3
Latent Heat (kJ/kg)	-	2470

2.2. Methodology

Computational Fluid Dynamics (CAD) is a branch of Fluid Mechanics. It calculates and analyzes problems involving fluid flows by using numerical analysis and algorithms of fluid mechanics. In the present study, ANSYS Fluent 15.0 software is used for numerical calculations. Numerical calculations are performed in three stages in ANSYS Fluent.

Pre-processing: In the pre-processing, the system was geometrically modeled in ANSYS Workbench and then the mesh structure was formed accordingly. Special attention was paid that the mesh structure would have been trapezoidal (triangular) and the skewness factor would have been less than 0.96. For the system, a high smoothing and a fine mesh size were used. The minimum size and edge length were selected as 0.10 mm and 5E-002 mm, respectively. The Patch Conforming Method was used in ANSYS meshing tool. The inflation layers have been added on the mesh structure of heat sink for a good approximation for natural convection. Two nested flow fields were created in the system and the mesh structure of the inner flow field was formed denser than that of the outer one. Approximately 5.000.000 elements and 1.300.000 node points were obtained on the model for each analysis. Details of the mesh structure are given in Figure 2.

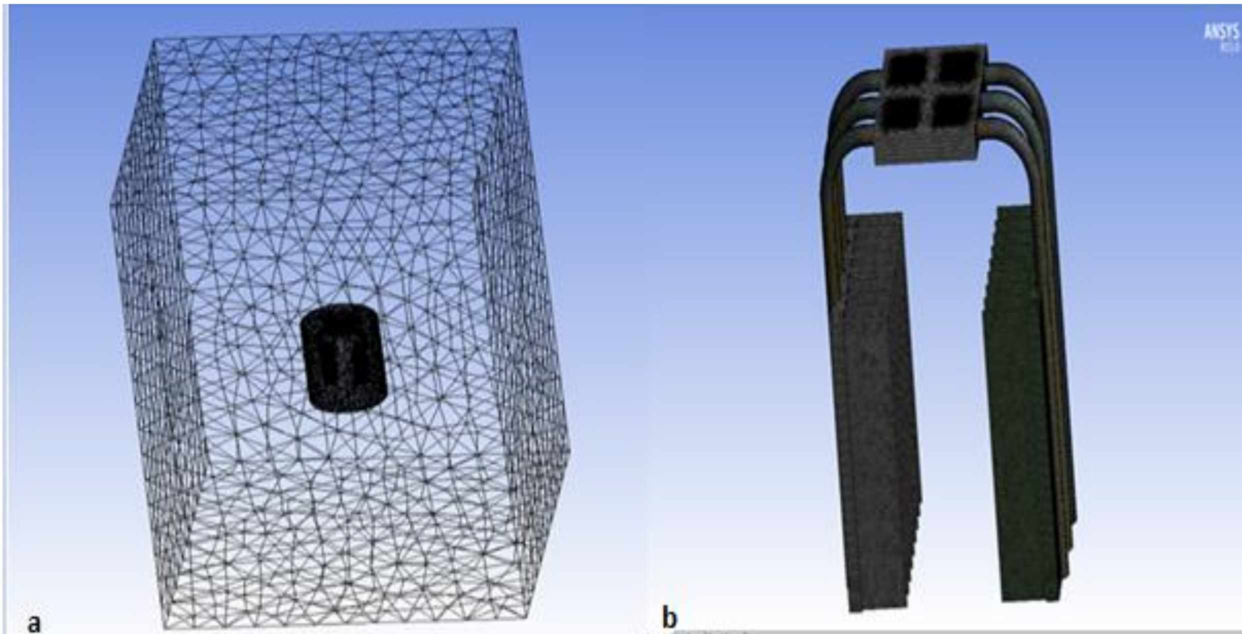

Figure 2. *Mesh generation* ***a)*** *with flow zone* ***b)*** *without flow zone of the whole geometry*

Solver: In the solver phase, boundary conditions were entered in solver and calculations were performed using Navier-Stokes equations. Navier Stokes equations consist of three equations: The continuity equation, the momentum equation and the energy equation. These are given in equations (1-5). In ANSYS Fluent, "Simple Method" and "Turbulent Mixing Length" model were used for the numerical calculations. The gravity is set in the negative vertical axis direction. The Coupled Pressure-Velocity Coupling scheme was used and gradient option was set to "Green-Gaused Nodes Based". For better accuracy, "the Body Forced Weighted Pressure Scheme" was set to take natural convection effects into account. The other discretion options were set to "Second Order Upwind".

Continuity Equation

$$\frac{\partial u}{\partial x} + \frac{\partial v}{\partial y} + \frac{\partial w}{\partial z} = 0 \qquad (1)$$

Momentum Equation

x- momentum

$$\rho\left(u\frac{\partial u}{\partial x}+v\frac{\partial u}{\partial y}+w\frac{\partial u}{\partial z}\right)=-\frac{\partial \rho}{\partial x}+\mu\left(\frac{\partial^2 u}{\partial x^2}+\frac{\partial^2 u}{\partial y^2}+\frac{\partial^2 u}{\partial z^2}\right) \quad (2)$$

y- momentum

$$\rho\left(u\frac{\partial v}{\partial x}+v\frac{\partial v}{\partial y}+w\frac{\partial v}{\partial z}\right)=-\frac{\partial \rho}{\partial y}+\mu\left(\frac{\partial^2 v}{\partial x^2}+\frac{\partial^2 v}{\partial y^2}+\frac{\partial^2 v}{\partial z^2}\right) \quad (3)$$

z- momentum

$$\rho\left(u\frac{\partial w}{\partial x}+v\frac{\partial w}{\partial y}+w\frac{\partial w}{\partial z}\right)=-\frac{\partial \rho}{\partial z}+\mu\left(\frac{\partial^2 w}{\partial x^2}+\frac{\partial^2 w}{\partial y^2}+\frac{\partial^2 w}{\partial z^2}\right) \quad (4)$$

Energy Equation

$$\left(u\frac{\partial T}{\partial x}+v\frac{\partial T}{\partial y}+w\frac{\partial T}{\partial z}\right)=\frac{1}{\alpha}+\mu\left(\frac{\partial^2 w}{\partial x^2}+\frac{\partial^2 w}{\partial y^2}+\frac{\partial^2 w}{\partial z^2}\right) \quad (5)$$

In the analyses, some assumptions were made for the heat pipe. They are listed below.

- Liquid flow is laminar incompressible and vapor is a saturated ideal gas.
- The flow is in steady-state conditions.
- All properties of the liquid is constant throughout the entire process.
- Condensation and evaporation occurs only in the liquid vapor interface.
- In the liquid-vapor interface, thermodynamic equilibrium is conserved.
- The heat pipe does not exchange any heat with the ambient environment, that is, it is adiabatic.
- Multi- phase model is selected for heat pipe calculations. In the absence of phase change of the interface, the heat flux must be continuous. So the fluid obeys stationary wall with no slip conditions.

Post-Processor: The findings were visualized in pro-processor. The temperature distributions of the system were obtained.

3. NUMERICAL ANALYSIS AND RESULTS

In the current study, numerical simulations were conducted at ANSYS Fluent to examine the thermal behavior of the system, which is designed for street illumination. After the program run, it was converged after approximately 4400 iterations. Figure 3 shows the convergence diagram of the analysis. At the end of calculations, the temperature distribution of the whole model was obtained at the given geometry and boundary conditions (Figure 4). According to this, the maximum temperature of each LED chip was 78.2 °C.

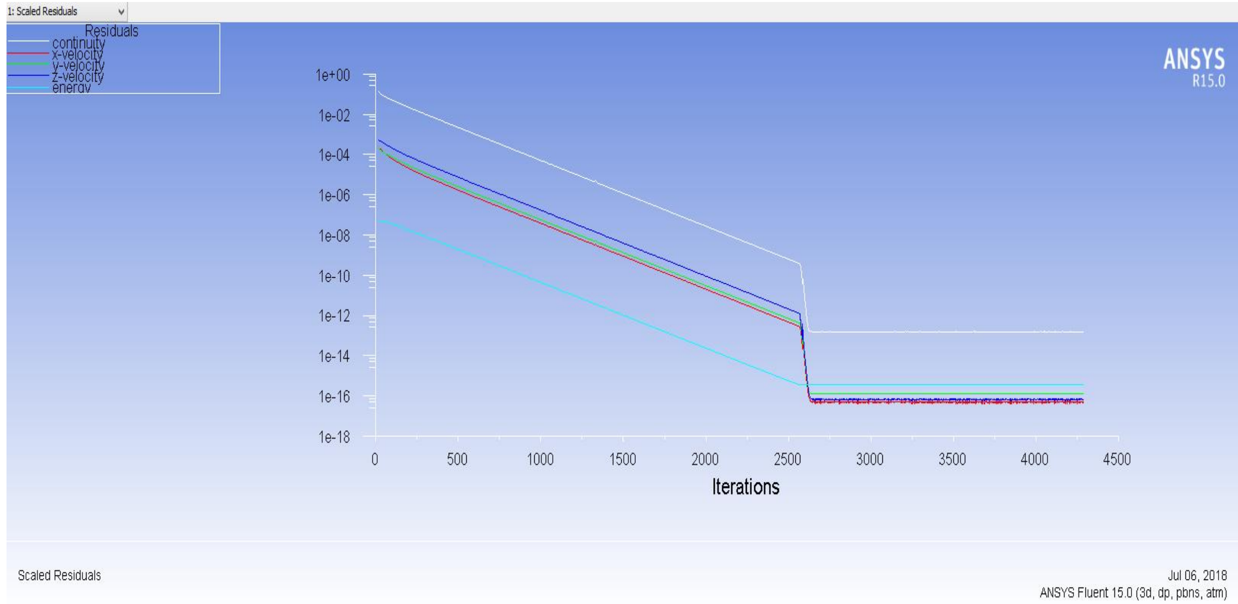

Figure 3. *Convergence diagram of thermal analysis in Fluent solver*

To examine the effect of the number of heat pipes on the temperature distribution of the whole system, single, double and quadruple heat pipes versions of the model were designed and each was numerically analyzed under the same boundary conditions. The temperature distributions obtained from the analyses are shown in Figure 5-7.

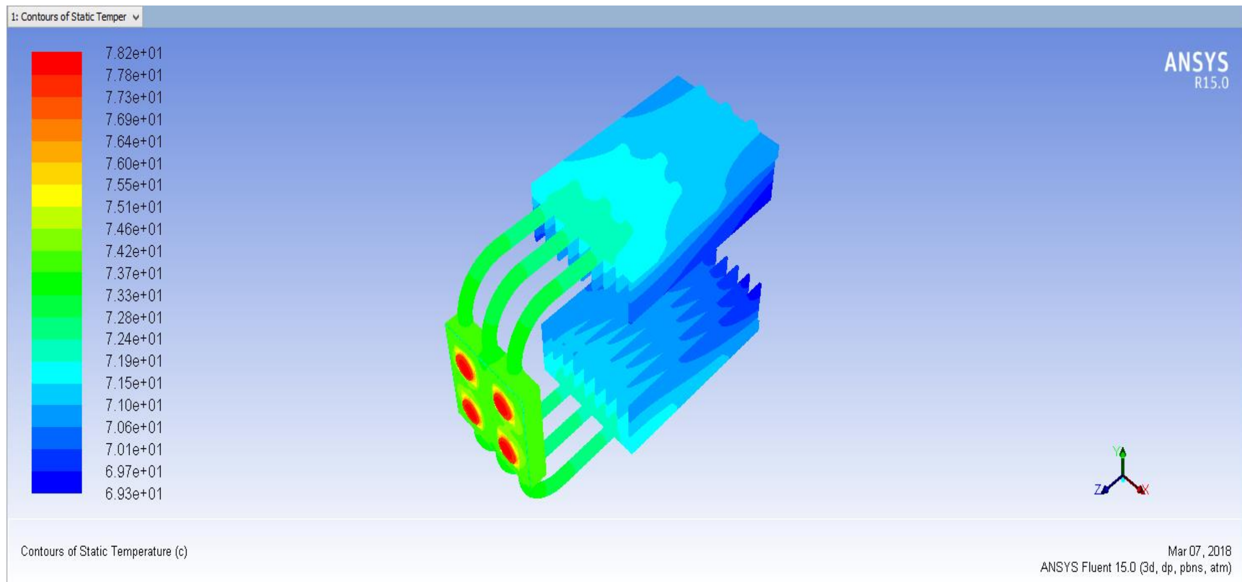

Figure 4. *Temperature distribution of the system for given boundary conditions*

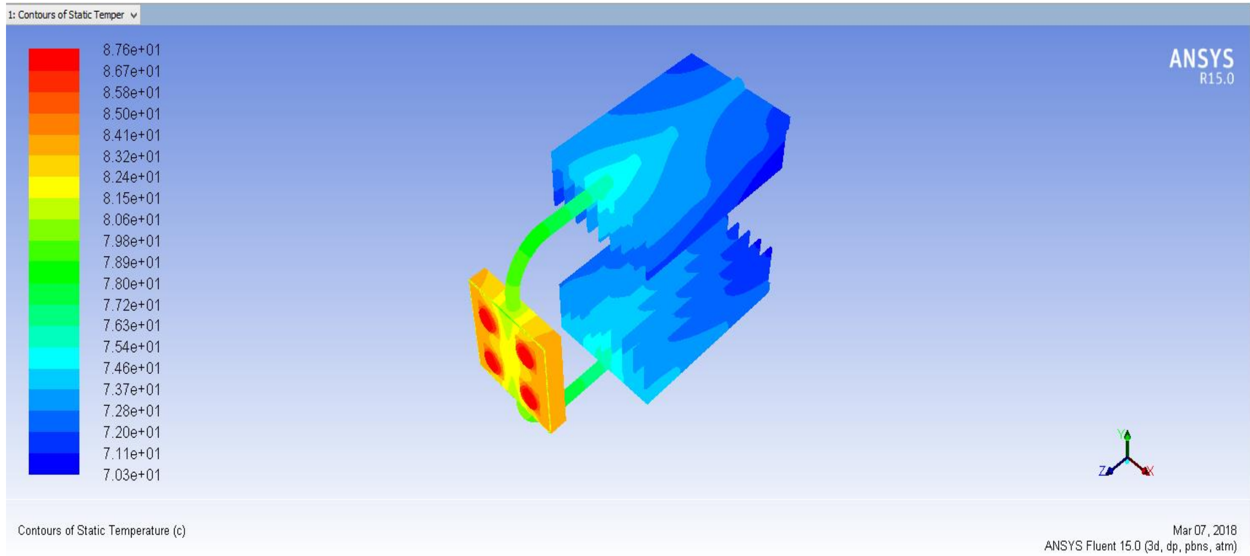

Figure 5. *Temperature distribution of the system with single heat pipe*

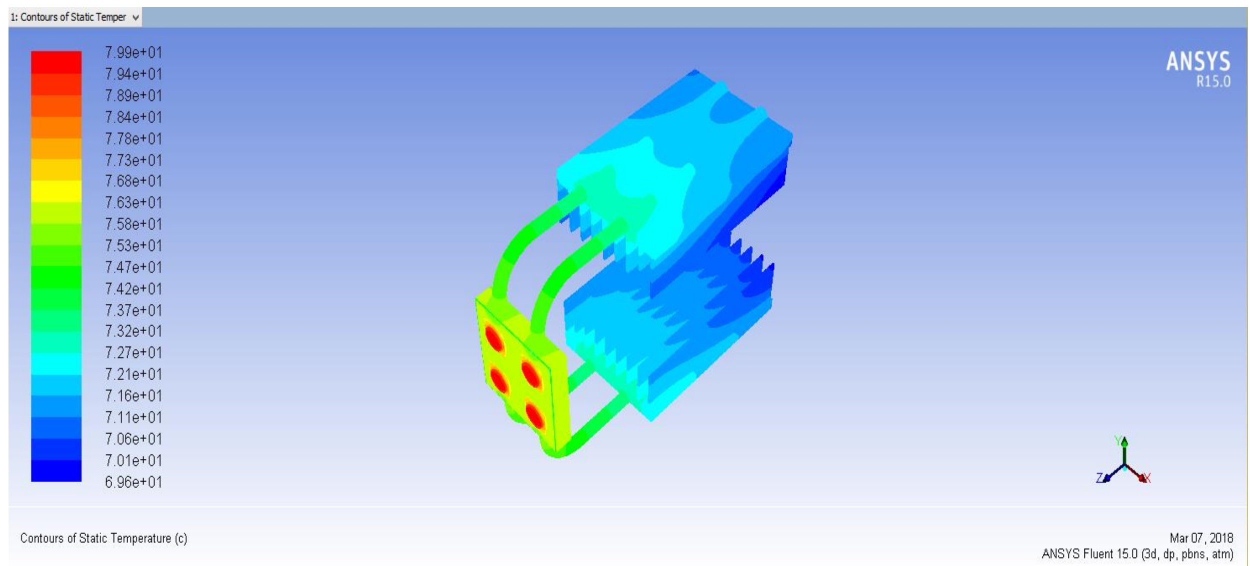

Figure 6. *Temperature distribution of the system with double heat pipe*

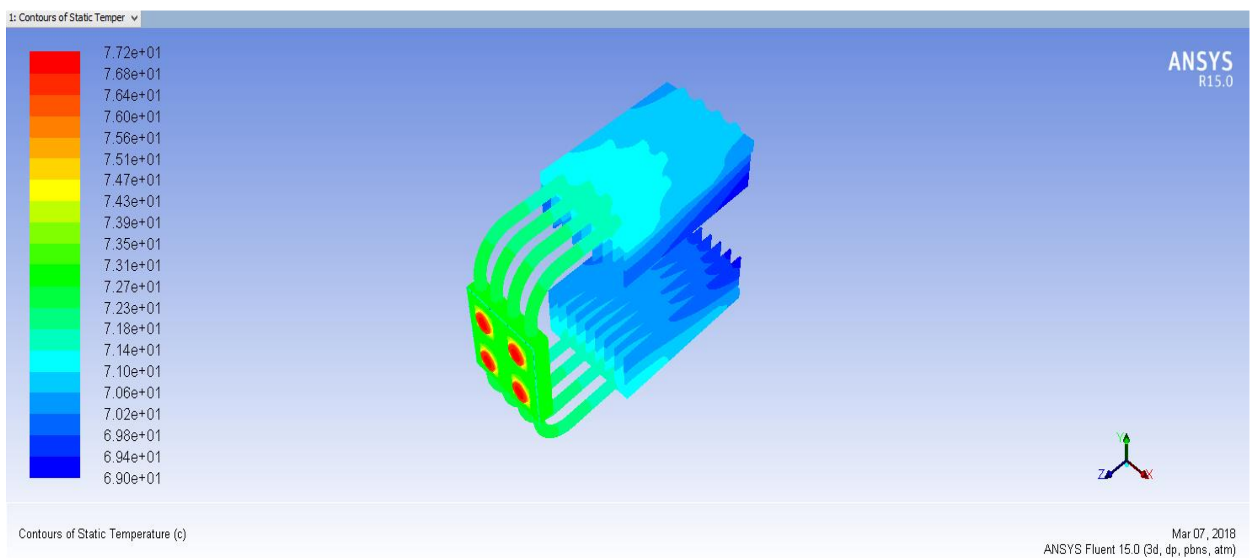

Figure 7. *Temperature distribution of the system with four heat pipe*

The results show that as the number of heat pipes increases, the maximum temperature of LED chip decreases and the maximum temperature of system with a single heat pipe is much higher than those of others. Heat pipe diameter is also one of the parameters that affect the maximum temperature. Numerical analyses of thermal behavior with various numbers of 8, 10, 12 and 14 mm diameter heat pipes were run. Figure 8 depicts the effect of the heat pipe diameter and number on the maximum temperature of the LED chip.

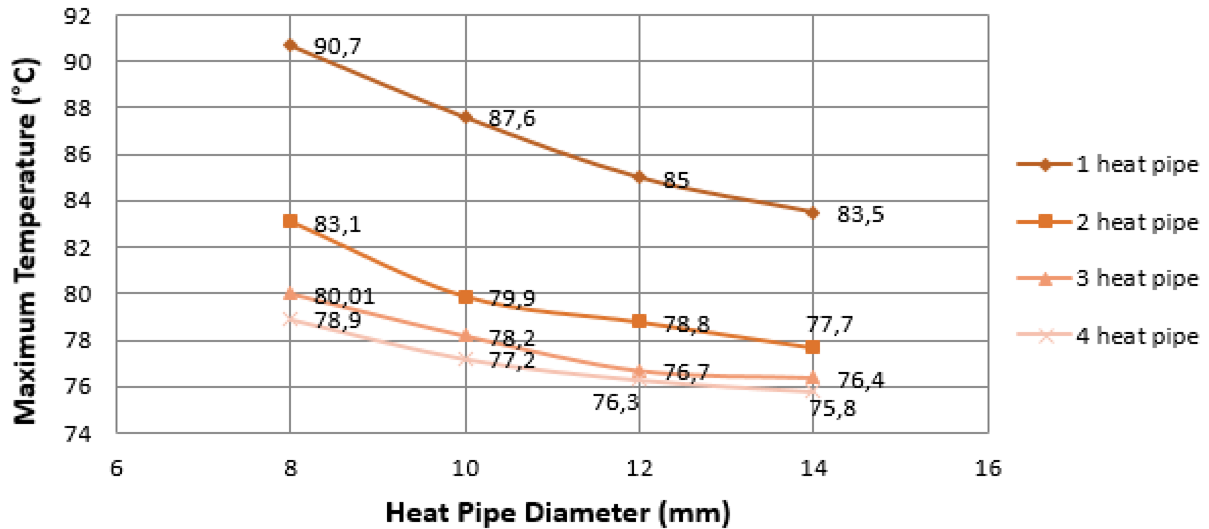

Figure 8. *Variation of maximum LED chip temperature with heat pipe diameter and number*

In calculations, firstly ambient temperature and heat load on LED chip were assumed to be 35 °C and 25 W respectively. Later different heat loads were applied to the LED chip to determine effect of the maximum temperature for ambient temperatures of 25 °C, 30 °C and 35 °C (Figure 9).

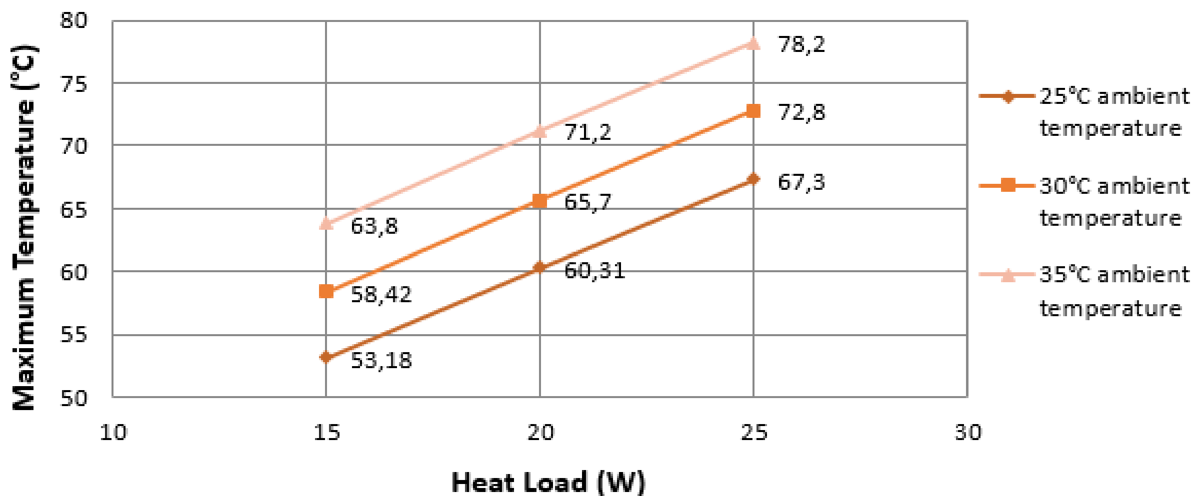

Figure 9. *Variation of maximum LED chip temperature with different heat load and ambient temperatures.*

In Figure 10, results of the investigation of the heat pipe's evaporator region and the condenser region lengths are presented. It is seen in the figure that, the maximum temperatures are almost the same for 80 mm and 100 mm evaporator lengths, whereas, it is only marginally lower for 120 mm evaporator length. However, the pattern is not the same for the length of the condenser region. It can be observed that, the maximum temperature decreases with the increasing condenser region length, at a rate of approximately 1 °C per 25 mm increment.

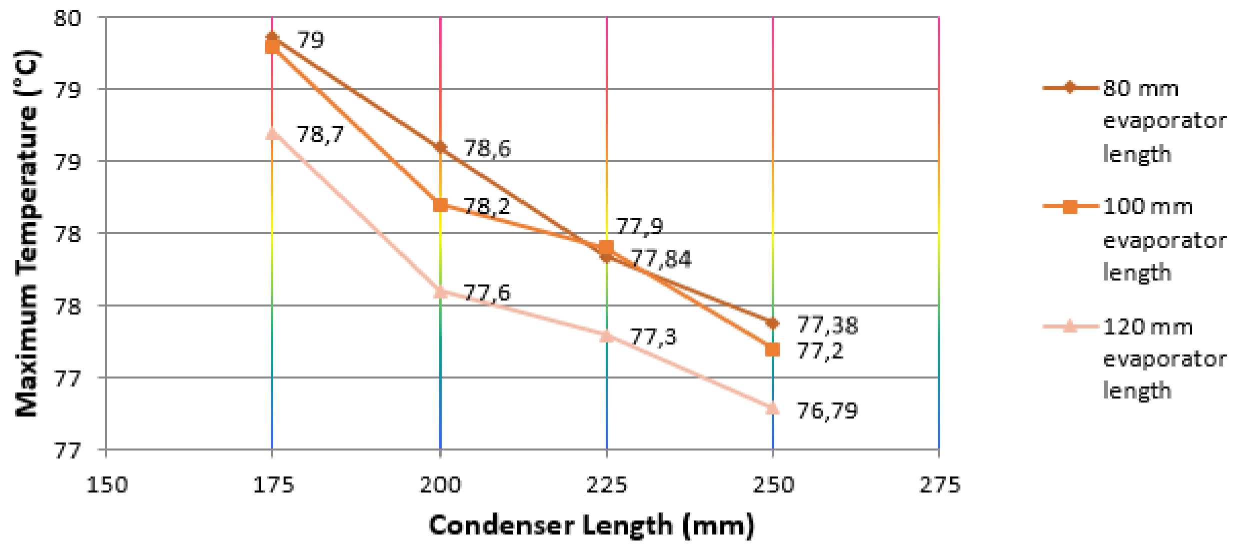

Figure 10. *Variation of maximum LED chip temperature with different evaporator and condenser length of heat pipe*

3.1 Thermal Resistance

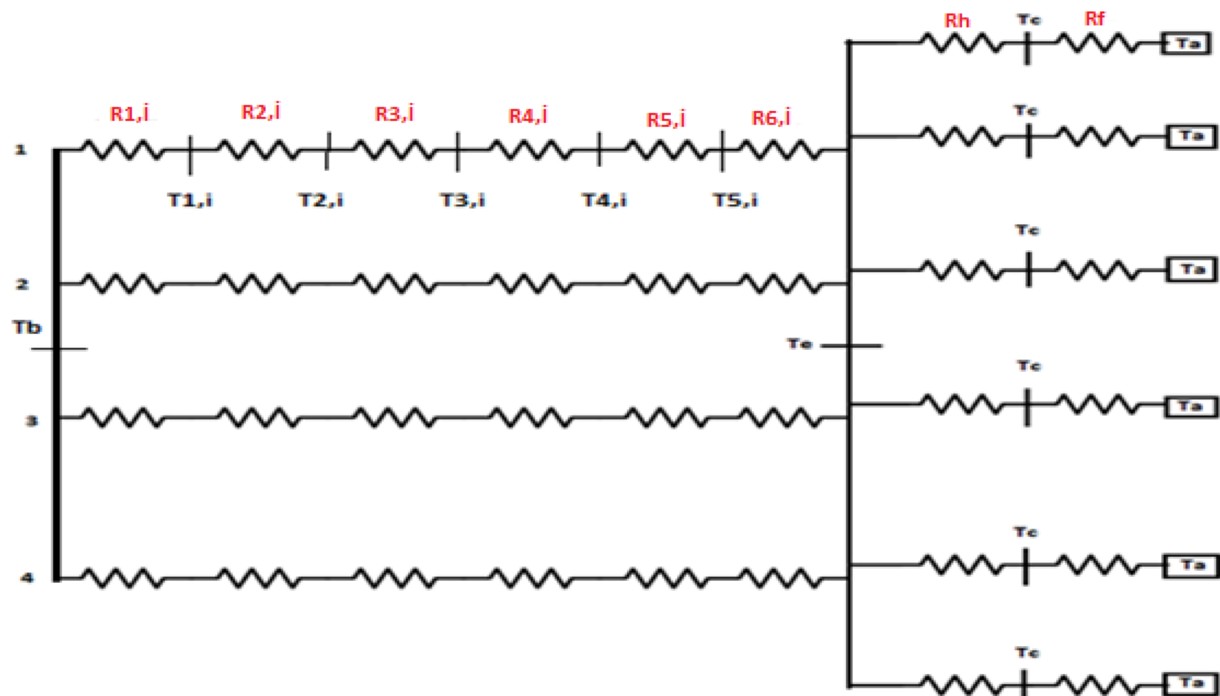

Figure 11. *Thermal resistance network model of designed geometry*

Thermal resistance network model of the designed system is shown in Figure 11. In the figure, maximum temperature of the LED chip is Tb, evaporator region temperature is Te, average temperature of the condenser region is Tc and ambient temperature is Ta. According to this model, the system is divided into two parts when calculating total thermal resistance. The first part from LED chip to heat sink is defined as R_{th1} and the second part from evaporator region to ambient is defined as R_{th2}. The total thermal resistance is calculated according to equation (6).

$$R_{th}=R_{th1}+R_{th2} \tag{6}$$

R_{th1} ve R_{th2} are calculated as in Eq. (7) and Eq. (8), respectively.

$$R_{th1} = \left(\sum_{i=1}^{4} \frac{1}{R_{LEDi}}\right)^{-1} \quad (7)$$

$$R_{th2} = \left(\sum_{i=1}^{6} \frac{1}{R_{h,i} + R_{f,i}}\right)^{-1} \quad (8)$$

The system was also analyzed under different boundary conditions. Total thermal resistance values were calculated in wind speeds ranging between 0.1 m/s and 1 m/s for different heat loads by using equation (6). In Figure 12, total thermal resistance values versus heat loads and wind speeds are plotted.

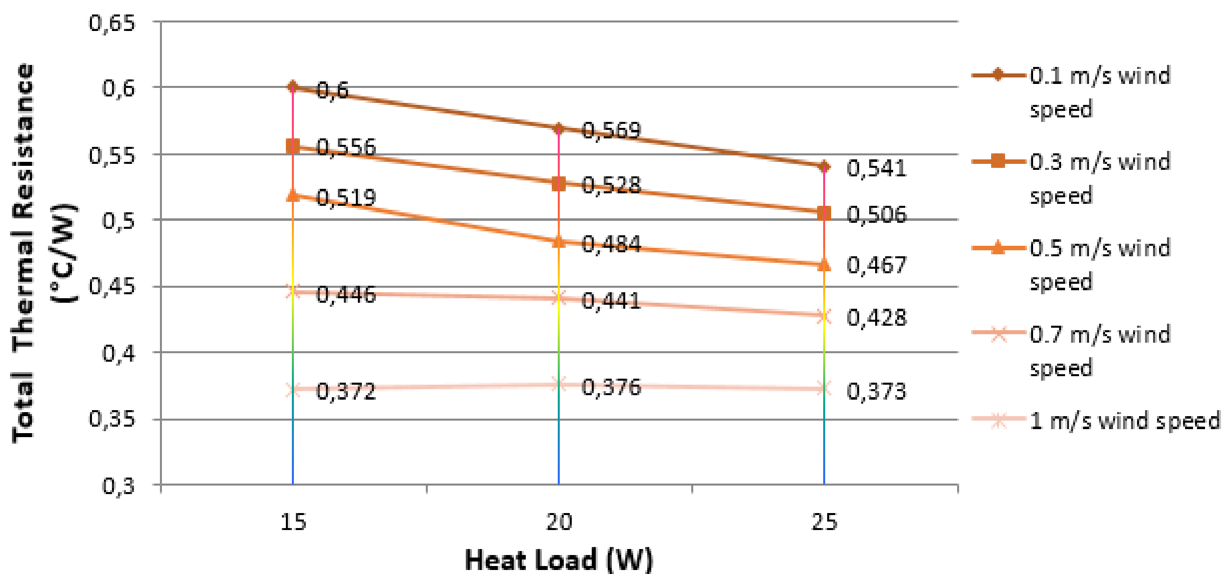

Figure 12. *Variation of thermal resistance with heat load and wind speed (at 35℃ ambient temperature)*

3.2. Material Effect on Maximum Temperature of LED’s

In this study, besides the heat pipe geometry and boundary conditions, the effects of the material selected for component manufacturing of the system was investigated. In electronic systems, aluminum and its alloys are generally used for heat sinks, it depends on the heat load though, In this study, heat sink materials of different heat absorption capabilities and coefficients of thermal conductivity, such as stainless steel (14 w/m.K), magnesium (79 W/m.K), aluminum (202 W/m.K) and copper (394 W/m.K) were used as heat sink materials. The temperature distributions obtained from the analyses for various heat sink materials are shown in Figure 15. Calculations show that magnesium, with a heat conductivity of 79 W /m.K, does not create much difference in heat distribution compared to aluminum and copper cooler plate (Figure 14). Magnesium is seen as a good alternative for heat sink material selection because it is a low density, light weight, heat resistant and highly corrosion-resistant material.

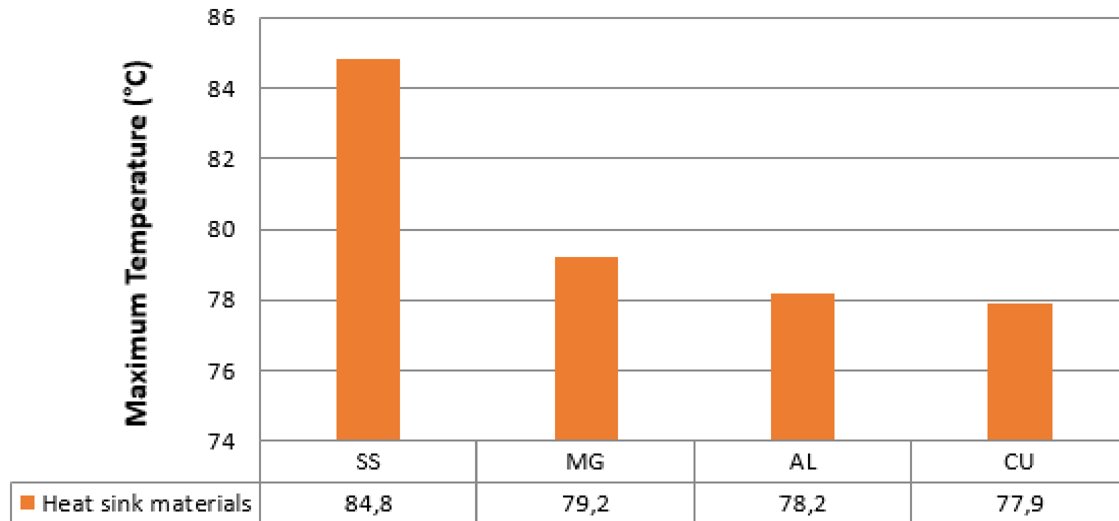

Figure 13. *Effect of heat sink materials on maximum LED chip temperature (SS-Stainless Steel, MG-Magnesium, Al-Aluminum, CU-Copper)*

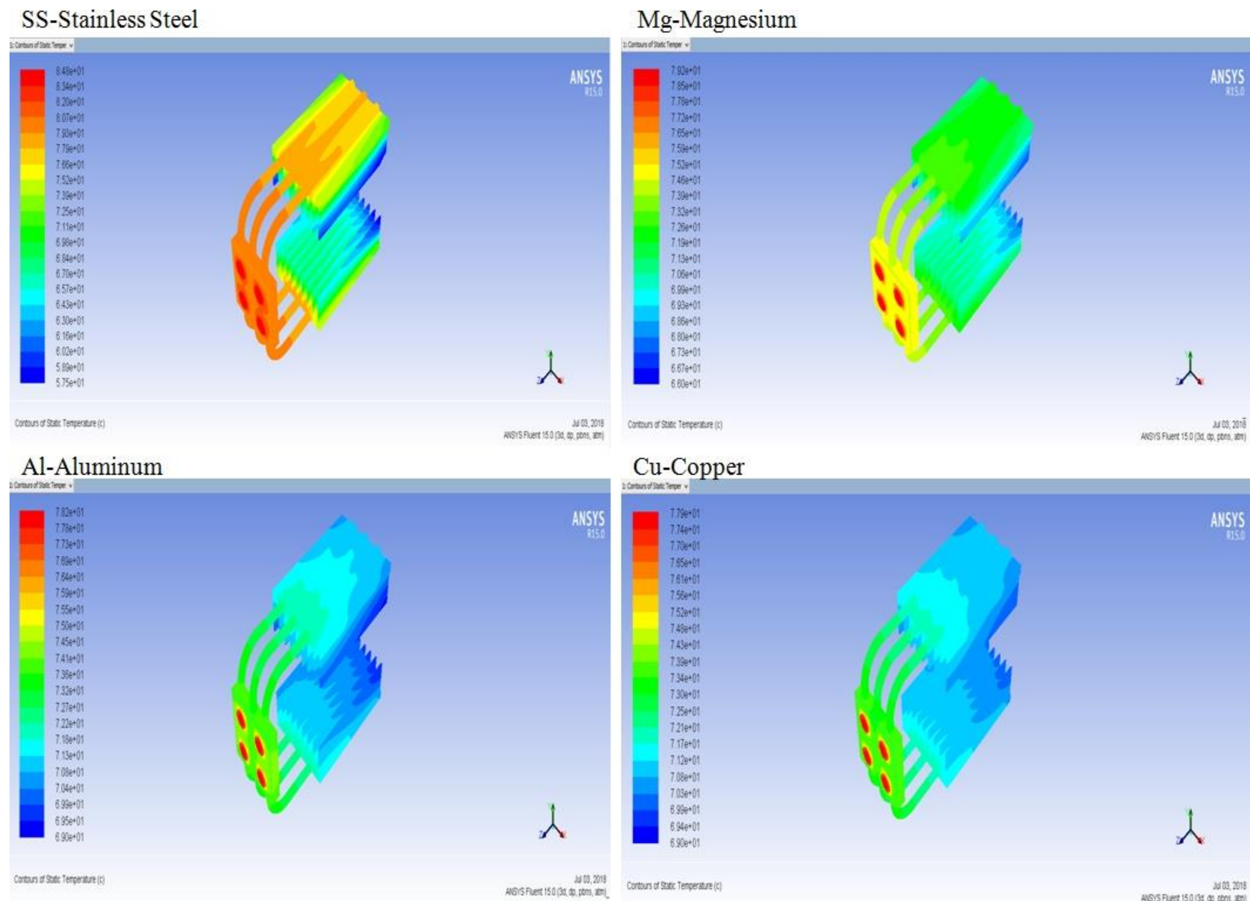

Figure 14. *Temperature distribution of the system for various heat sink materials.*

In LED packages, silicon, silicon carbide and sapphire (Al_2O_3), which have different thermophysical properties, were used as die materials. The temperature distributions obtained from the analyses for various LED die materials is shown in Figure 16. Despite the difference between the thermal conductivities of the materials, no significant difference between the maximum LED temperatures they produced was observed (Figure 15).

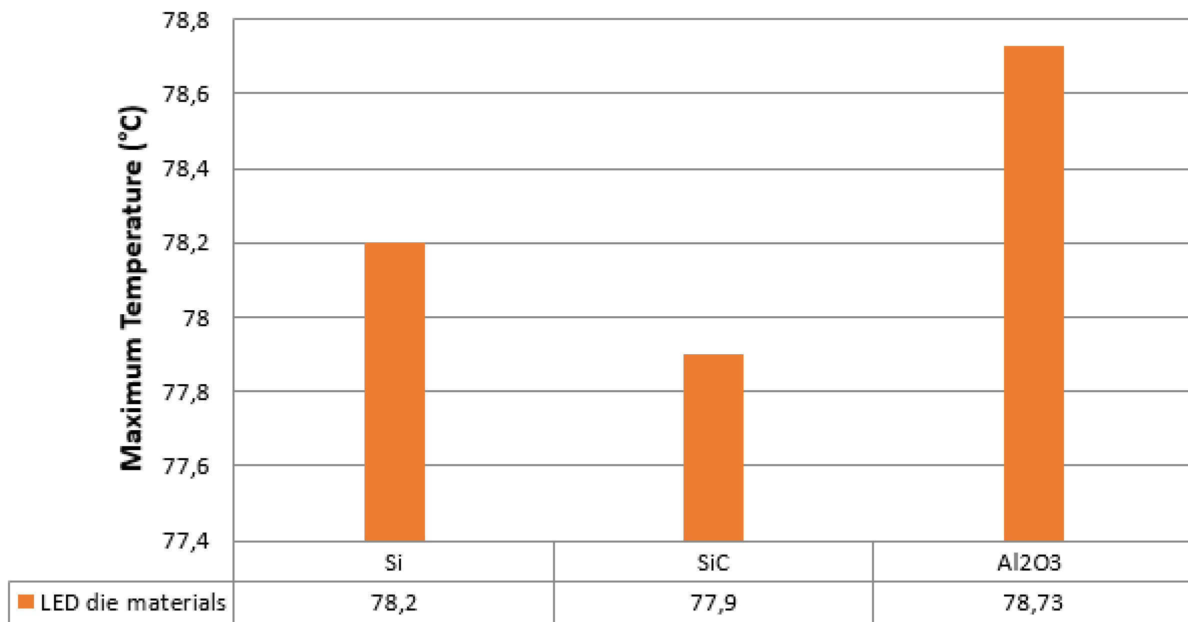

Figure 15. *Effect of LED die materials on maximum LED chip temperature (Si-Silicon, SiC-Silicon Carbide,* Al_2O_3*-Sapphire)*

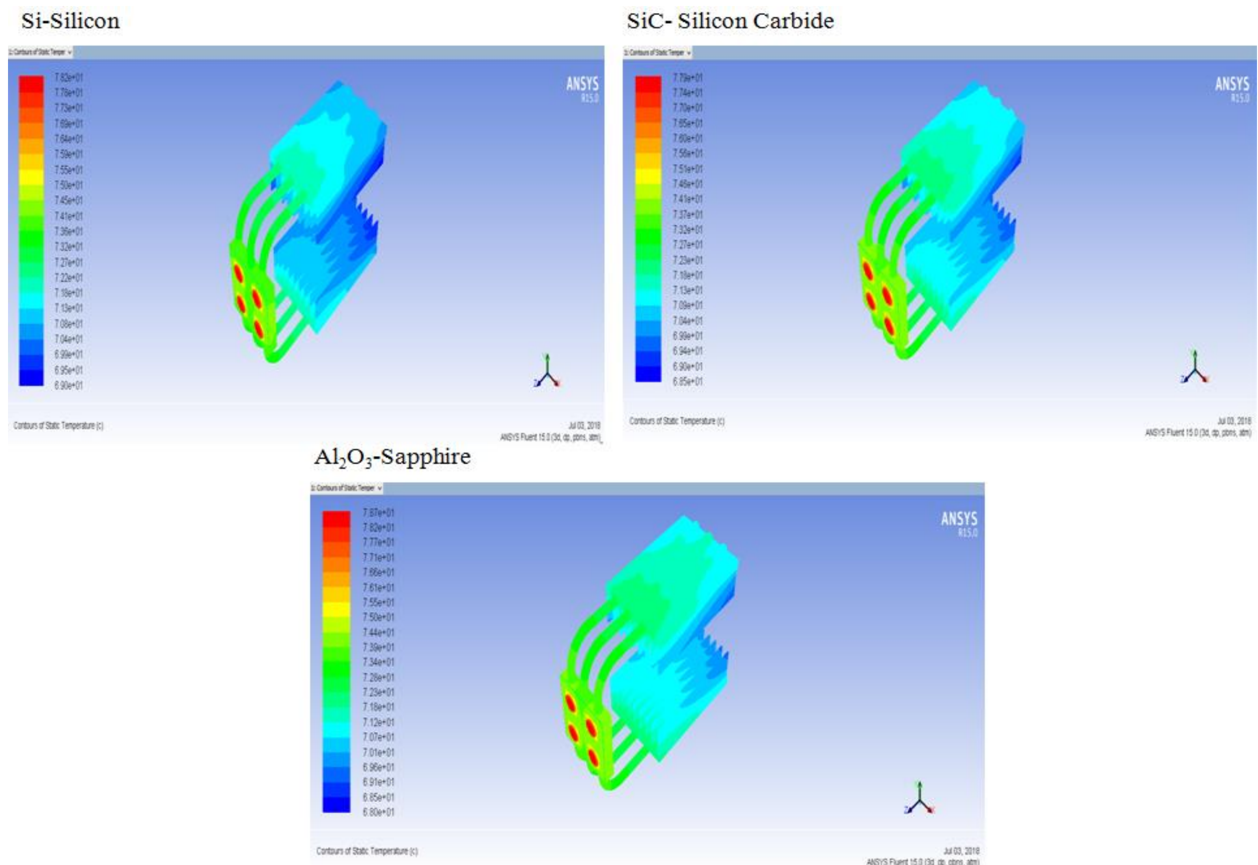

Figure 16. *Temperature distribution of the system for various LED die materials*

In order to create an electrical circuit in the LED packages, electronic and printed circuit boards such as Al_2O_3 DBC, Si_3N_4 AMB, AlN DBC and IMS (Insulated Metal Surface) are used. These are produced by different methods and have different characteristics. According to the properties of electronic and printed circuit boards given in Table 1, numerical calculations were performed for each circuit board in ANSYS Fluent. During the process, all the other geometric and boundary conditions of the system were kept

constant. The temperature distributions obtained from the analyses for various electronic/printed circuit board materials are shown in Figure 18. Effect of the electronic/printed circuit board on the maximum temperature is determined as shown in Figure 17. Results show that the maximum temperature of the system is the highest in the model using IMS printed circuit board, which has the lowest thermal conductivity. As the heat conductivities of electronic/printed circuit boards increase, it was observed that, generally, the maximum temperature in the system decreases. However, there was a difference of less than 1 °C between the maximum temperatures of the models with Al_2O_3 DBC (coefficient of thermal conductivity = 24W/m.K) and models with AlN DBC of (coefficient of thermal conductivity = 180W/m.K).

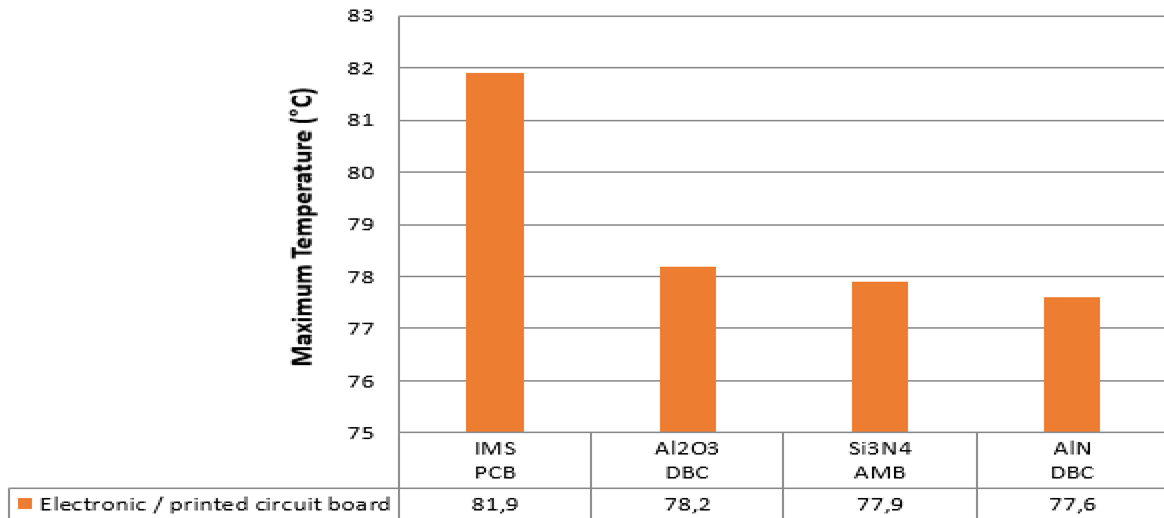

Figure 17. *Effect of electronic/printed circuit board on maximum LED chip temperature*

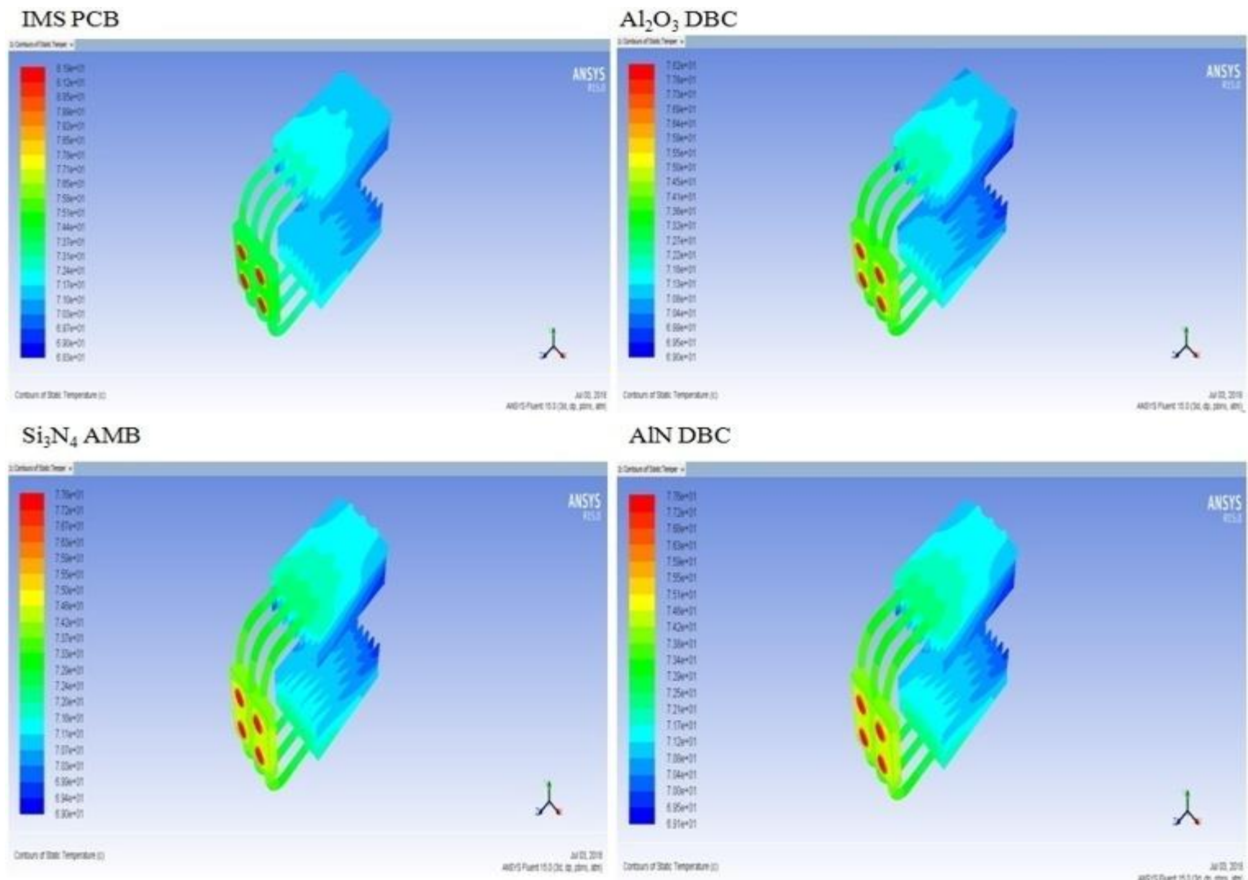

Figure 18. *Temperature distribution of the system for various electronic/printed circuit board materials*

4. CONCLUSION

After analyzing the system in this study, which was designed to dissipate the heat generated in high power LEDs, it was observed that heat pipe geometry has an effect on the temperature distribution of the entire system. Also taking cost control into account, the optimum number, diameter and length of the heat pipes were determined. Results show that, if 2 or 3 heat pipes with diameters 10 or 12 mm's are used, maximum temperature occurring in the LED stays within foreseeable limits. It was observed that, the effect of the length of the heat pipe's condenser region on the maximum temperature of the LED chips was at most 2 ºC. That is, the difference between the top value and the bottom value of the maximum temperature was below 2 ºC. Optimum materials to be used in LED package components were determined by trying and analyzing different materials, each having different thermophysical properties such as coefficient of thermal conductivity, density and specific heat. The results obtained reveal that, thermal conductivity affects the maximum temperature up to some point. After that point, higher thermal conductivity does very little effect on the maximum temperature. For example, stainless steel, magnesium,aluminum and copper were used as heat sink materials. When stainless steel, whose thermal conductivity is 14 W/m.K, was used, the maximum LED temperature was 84.8 °C. Magnesium, having a thermal conductivity of 79 W/m.K, pulled this temperature down to 79.2 °C. From this point on, aluminum (202 W/m.K) and copper (394 W/m.K) did not bring a significant improvement over magnesium in terms of maximum LED temperature. Similarly, among the electronic / printed circuit boards with different thermal conductivities, usage of IMS PCB, having a thermal conductivity of 1.1 W/m.K, resulted in a maximum LED temperature of 81.9 °C On the other hand, in the case of Al_2O_3 DBC with its thermal conductivity of 24 W/m.K, the maximum LED temperature dropped to 78.2 °C. Neither Si_3N_4 nor AlN DBC, despite having higher thermal conductivities (80 W/m.K and 180 W/m.K, respectively), provided a more than 1 °C reduction in the maximum LED temperature, compared to Al_2O_3 DBC. Since the system was designed to be used for street illumination (so, outdoor usage), ambient temperature and wind speed were also taken into account in the computations. Accordingly, system simulation was run under various ambient temperature and various wind speed conditions and the effects of these parameters on the system's thermal behavior were examined. For the ambient temperature, the simulation was run with 25 °C, 30 °C and 35 °C ambient temperatures, for which, the resultant maximum temperatures in the LED chip were 67.3 °C, 72.8 °C and 78.2 °C, respectively. Expectedly, maximum temperature in the LED chip dropped with decreasing ambient temperature. For the wind speed, analyses revealed that total thermal resistance decreased with increasing wind speeds. For the same LED chip, when 0.1 m/s, 0.3 m/s, 0.5 m/s, 0.7 m/s and 1 m/s were entered as different wind speeds and simulations were run, total thermal resistance was changing from 0.541 °C/W to 0.373 °C/W with the increasing wind speed. The related results for different thermal loads are given in Figure 9.

CONFLICTS OF INTEREST

No conflict of interest was declared by the authors.

REFERENCES

[1] Internet: USA, In Indiana University of Pennsylvania. https://www.iup.edu/energymanagement/howto/led-lighting-benefits.html , (2018).

[2] Arik, M., Prtroski, J., Weaver, S., “Thermal challenges in the future generation solid state lighting applications: light emitting diodes”, International Packaging Technical Conference, Hawaii, 113-120, (2002).

[3] Gu, Y., Narendran, N., “A non-contact method for determining junction temperature of phosphor-convened white LEDs”, Third international conference on solid state lighting, San Diego, 5187: 107–114, (2004).

[4] Hu, J.S., Yang, L.Q., Shin, M.W., "Mechanism and thermal effect of delamination in light-emitting diode packages", Microelectronics Journal, 38(2): 157–163, (2007).

[5] Wang, J.C., Huang, H.S., Chen, S.L., "Experimental investigations of thermal resistance of a heat sink with horizontal embedded heat pipes", International Communications in Heat and Mass Transfer, 34(8): 958-970, (2007).

[6] Shen, S.C., Huang, H.J., Shaw, H.J., "Design and estimation of a MCPCB-flat plate heat pipe for LED array module", International Conference on Mechatronics and Automation, Takamatsu, 158-163, (2013).

[7] Tang, Y., Ding, X., Li, Z., Li, B., "A high power LED device with chips directly mounted on heat pipes", Applied Thermal Engineering, 66: 632-639, (2014).

[8] Moon, S.H., Park, Y.W., Yang, H.M., "A single unit cooling fins aluminum flat heat pipe for 100W socket type COB LED lamp", Applied Thermal Engineering, 126: 1164-1169, (2016).

[9] Wang, M., Tao, H., Sun, Z., Zhang, C., "The development and performance of the high power LED radiator", International Journal of Thermal Sciences, 113: 65-72, (2017).

[10] Carbajal, G., Sobhan, C.B., Queheillalt, D. T., Wadley, H. N., "A quasi-3D analysis of the thermal performance of a flat heat pipe", International Journal of Heat and Mass Transfer, 50: (21-22), 4286-4296, (2007).

[11] Naveenkumar, Ch., Vijay Kumar P., Dilip Kumar D., "Simulation and CFD analysis of heat pipe with different wick geometry using CFX", International Journal of Thermal Technologies, 5(3): 210-213, (2015).

[12] Annamalai, S.A., Ramalingam, V., "Experimental investigation and CFD analysis of an air cooled condenser heat pipe", Thermal Science, 15(3): 759-772, (2011).

[13] Suresh, Z.V., Bhramara, B., "CFD Analysis of single turn pulsating heat pipe", International Journal of Scientific & Engineering Research, 7(6): 238-244, (2016).

[14] Asmaie, L., Haghshenasfard, M., Mehrabani-Zeinabad, A., Esfahany, M.N., "Thermal performance analysis of nanofluids in a thermosyphon heat pipe using CFD modeling", Heat and Mass Transfer, 49(5): 667-678, (2013).

[15] Ashish R., Chaudhari, Bhosale S.Y., "CFD validation and experimental investigation of circular heat pipe using hybrid nanofluid", International Journal of Innovative Research in Science, Engineering and Technology, 5(9): 16058-16064, (2016).

[16] Lin, Z., Wang, S., Shirakashi, R., Zhang, L.W., "Simulation of a miniature oscillating heat pipe in bottom heating mode using CFD with unsteady modeling", International Journal of Heat and Mass Transfer, 57(2): 642-656, (2013).

[17] Wang, J., Ma, H., Zhu, Q., "Effects of the evaporator and condenser length on the performance of pulsating heat pipes", Applied Thermal Engineering, 91: 1018-1025, (2015).

[18] Dev, K., Budania, B., "Simulation and modeling of heat pipe", International Journal of Technical Research, 5(1), (2016).

[19] Elnaggar, M.H., Abdullah, M.Z., Mujeebu, M.A., "Experimental analysis and FEM simulation of finned U-shape multi heat pipe for desktop PC cooling", Energy Conversion and Management, 52(8-9): 2937-2944, (2011).